

Article

# Design and Production of Animated Image Photovoltaic Modules

Yu-Chih Ou <sup>1</sup>, Hsin-Yu Wu <sup>2</sup>, Chia-Hsun Hsu <sup>3</sup>, Yeu-Long Jiang <sup>2</sup> and Shui-Yang Lien <sup>1,3,\*</sup> 

<sup>1</sup> Department of Electrical Engineering, Da-Yeh University, Chunghua 51591, Taiwan; yuchinoh@gmail.com

<sup>2</sup> Graduate Institute of Optoelectronic Engineering and Department of Electrical Engineering, National Chung Hsing University, Taichung 40227, Taiwan; xinmarchentic@gmail.com (H.-Y.W.); yljiang@nchu.edu.tw (Y.-L.J.)

<sup>3</sup> Department of Materials Science and Engineering, Da-Yeh University, Chunghua 51591, Taiwan; cstcaptive@gmail.com

\* Correspondence: syl@mail.dyu.edu.tw; Tel.: +886-04-851-1888 (ext. 1760)

Received: 30 September 2017; Accepted: 24 October 2017; Published: 26 October 2017

**Abstract:** This paper develops fifth-generation-sized silicon thin-film tandem photovoltaic (PV) modules with animated images. Front PV cell stripes are created using a laser scribing technique, and specially edited and shifted images are printed onto the back glass. After encapsulating the front PV module with the back glass, the animated image effect can then be clearly seen from various positions. The PV module that can display three images has a stabilized power output of 87 W. The remarkable features of this module such as its animated image display, semitransparency, and acceptable power loss give it great potential for use in building-integrated photovoltaics. This paper could help improve the aesthetic appearance of PV modules, which may increase users' or architects' willingness to install PV modules on buildings.

**Keywords:** animated image; photovoltaic (PV) module; semitransparency; building-integrated photovoltaic

## 1. Introduction

Building-integrated photovoltaic (BIPV) has gained great attention in recent years because it can serve as a building envelope material. Numerous market research studies have forecasted the rapid expansion of the BIPV market; a report released by SolarPower Europe indicated that the total global installed solar capacity would grow from 306.5 GW in 2016 to 700 GW in 2021 [1]. Conventional silicon wafer-based solar cells have high power conversion efficiency, but they are only selected to be integrated on rooftops in BIPV applications because of the limitations of their optically opaque appearance. In contrast, silicon thin-film PV modules can be made transparent with acceptable power loss using a laser scribing technique [2–4], and these so-called “see-through” PV modules have started to be integrated into the windows and curtains of buildings.

Despite the development of see-through modules, they still have a plain appearance. We aim to develop a PV module with animated images that are either based on scanimation or what is also referred to as the moiré animation technique [5–9]. Scanimation comprises a vertical bar pattern superimposed on top of a series of fragmented vertical segments of an image. When the top pattern moves horizontally, the bars or strips obscure each key frame (phase of movement) while revealing another, thus showing a looping animation.

This paper developed animated image silicon thin-film tandem PV modules. The design concept and fabrication process of the PV modules are indicated. The actual fifth-generation-sized (1.1 × 1.4 m<sup>2</sup>) animated module was installed, and the change in image caused by the different viewing angles to the PV module is demonstrated. Finally, the photovoltaic performance of the animated image PV module is also discussed.

## 2. Materials and Methods

The schematic structure of an animated image PV module is shown in Figure 1. The module consists of a series-connected silicon tandem cell at the front, encapsulated with back protective glass by ethylene vinyl acetate (EVA). The design and fabrication are described below. The structure of the silicon tandem solar cell was glass/SnO<sub>2</sub>:F (800 nm)/hydrogenated p-i-n amorphous silicon (300 nm)/hydrogenated microcrystalline p-i-n silicon (1750 nm)/ZnO:B (60 nm)/silver back contact (120 nm). The silicon tandem cell was series-connected using the standard laser processes known as P1 (ablated the front electrode), P2 (ablated the silicon films), and P3 (ablated the back electrode and silicon films) scribing techniques [10–12]. The cell width created by P1, P2 and P3 processes was 9 mm. The subsequent laser scribing step (P4) patterned see-through lines in orthogonal direction of P1, P2 and P3 lines to create stripes or bars on the PV module, as shown in Figure 2a. According to the number of animated images desired, the relationship between the widths of the stripes and the intervals (Figure 2b) was given as:

$$d_1 = (n - 1)d_2. \quad (1)$$

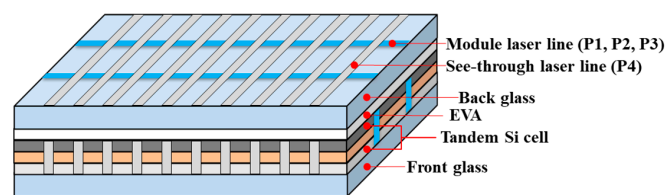
where  $d_1$  was the PV cell stripe width (period of the P4 lines),  $d_2$  was the P4 line width (30  $\mu\text{m}$  patterned in a single time), and  $n$  was the desired image number. The transmittance of the module was defined as:

$$\text{Transmittance (\%)} = \frac{d_2}{d_1 + d_2} \times 100\%. \quad (2)$$

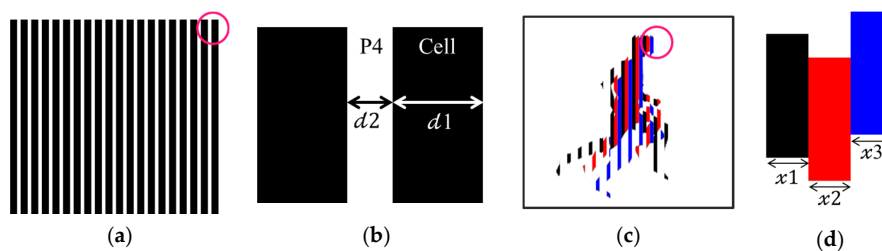
All the laser scribes were carried out by back scribing (i.e., through the glass side) [13,14]. Afterward, the images desired to be shown on the PV module were edited using computer software to appear as vertical stripes and each image was horizontally shifted. Figure 2c shows an example of this, in which three images are edited and shifted. In Figure 2d, every image stripe width ( $x_1$  to  $x_3$ ) was set to the same, and this satisfied the following equation:

$$x_1 = x_2 = x_3 = d_2. \quad (3)$$

The edited images were then inkjet-printed on a back protective glass. Finally, the front PV cell was EVA-encapsulated with the back glass. The fabrication of the animated image PV module was finished. The current–voltage (I–V) characteristics of the PV modules were measured at AM1.5G (1000 W/m<sup>2</sup>) using a solar simulator.



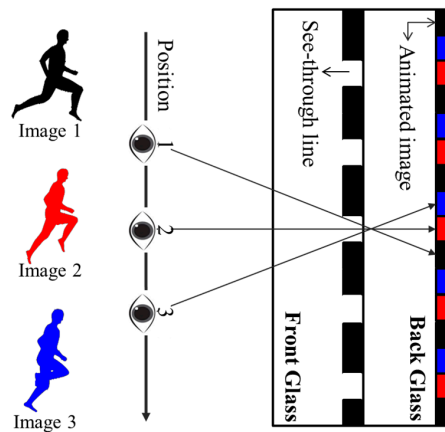
**Figure 1.** Schematic structure of the animated image photovoltaic (PV) modules.



**Figure 2.** (a) Front PV cell scribed by a P4 laser; (b) cell stripe width and P4 laser line width; (c) edited and shifted images on back glass; and (d) stripe widths for different images.

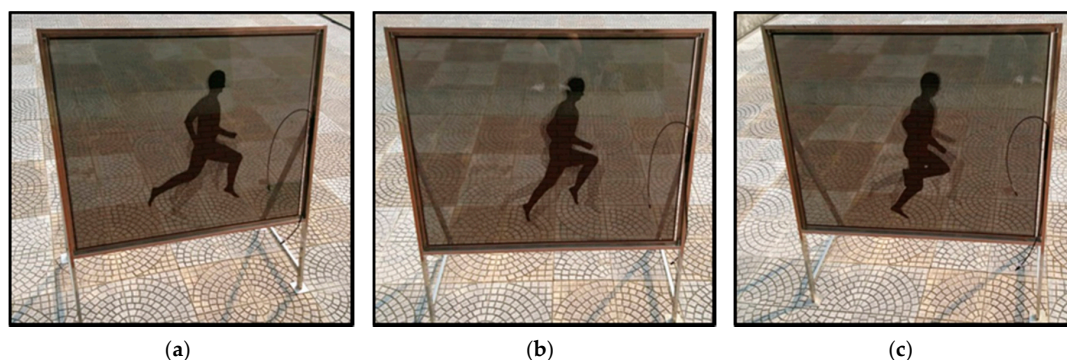
### 3. Results and Discussion

Figure 3 shows a scheme of the change in the image display on the PV module observed at different position angles. Based on the width design shown in Equations (1) and (3), the front PV cell stripe will reveal one kind of image at a time and hide the others. Therefore, observing the module from positions 1, 2, and 3 shows different images. It is inevitable that some overlap will be observable between the images, but this will be reduced as the distance between the observer and module increases.



**Figure 3.** Scheme of the image display on the animated image PV module at different viewing position angles.

Figure 4 shows the actual  $1.1 \times 1.4 \text{ m}^2$  fifth-generation-sized animated image PV modules corresponding to Positions 1, 2, and 3, as depicted in Figure 3. The viewing angles of Images 1, 2 and 3 were  $20^\circ$ ,  $0^\circ$  and  $-20^\circ$ , respectively. The Equation (3) is valid when the angle is  $0^\circ$ . For other angles, the overlap of the images will be observable depending on the distance between see-through line and animated image. The PV module is semitransparent because of the P4 see-through lines. This work uses three images, which corresponds to a module transmittance of approximately 33%. Overall, images can be clearly distinguished even though there are some slight image overlaps. When an observer moves from Position 1 to Position 3, continuously acting images can be observed.



**Figure 4.** Appearance of the fifth-generation-sized animated image PV modules observed at (a) Position 1; (b) Position 2; and (c) Position 3.

Figure 5 shows a comparison of the I–V characteristics between the animated image silicon tandem PV module and the standard opaque module, which had been fabricated in the same manner, except without P4 laser scribing. The detailed photovoltaic parameters of the modules such as the maximum power output ( $P_{\text{max}}$ ), open-circuit voltage ( $V_{\text{oc}}$ ), short-circuit current ( $I_{\text{sc}}$ ), fill factor

(FF), and conversion efficiency are also indicated. As the a-Si:H contained solar cells will suffer from well-known light-induced degradation, standard light-soaking tests were performed on the PV modules for 1000 h at 60 °C in accordance with IEC61647 [15] to obtain the stabilized PV module performance. It can be seen that compared to the standard module, the animated image PV module shows a 40% decrease in power output, from 144.9 to 87.6 W. This loss mainly results from the area loss of the silicon active layers, which is about 33% in this work. This is also directly reflected in the 35% decrease of  $I_{sc}$ . The remaining 5% loss may be attributed to the laser scribing damage to the silicon layers, which leads to decreases in  $V_{oc}$  and FF. Therefore, this result indicates that the most efficient method of reducing power loss is decreasing the ablation area, which in turn means less transparency. This can be done by increasing the image number. For example, if the image number increases to ten, the transparency will be 10% with an acceptable power loss of about 15–20%, as observed in a typical see-through PV module.

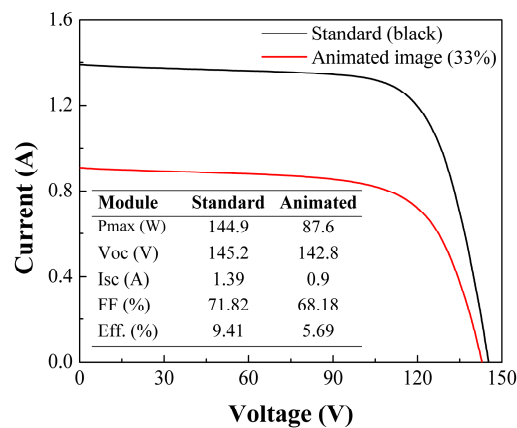


Figure 5. Current-voltage (I–V) characteristics of standard and animated image PV modules.

Figure 6 shows the performance of the standard PV module and a 33%-transmittance animated image PV module as a function of the irradiance. It can be seen that at an irradiance of approximately 250 W/m<sup>2</sup>, the  $V_{oc}$  and FF of the animated image PV module reach greater than 90% of their standard value (at 1000 W/m<sup>2</sup>). This confirms that the animated image PV module still has high maintenance of  $V_{oc}$  and FF in weak light conditions, which is the most remarkable feature of silicon thin-film solar cells. The  $I_{sc}$  of the animated PV modules again exhibits a slope approximately 1/3 smaller than that of the standard PV module due to the ablation loss of the silicon active layer. This result is helpful for evaluation of the performance of PV modules with different tilt angles ( $\theta_t$ ). When the tilt angle changes, the irradiance ( $I_r$ ) on the module will be varied according to  $I_r = I_0 \times \cos\theta_t$ , where  $I_0$  is the applied irradiance. Then the corresponded cell performance can be found.

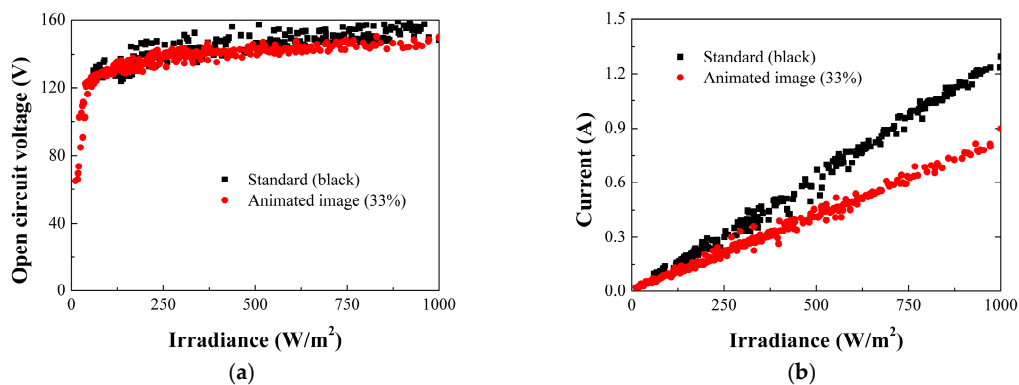
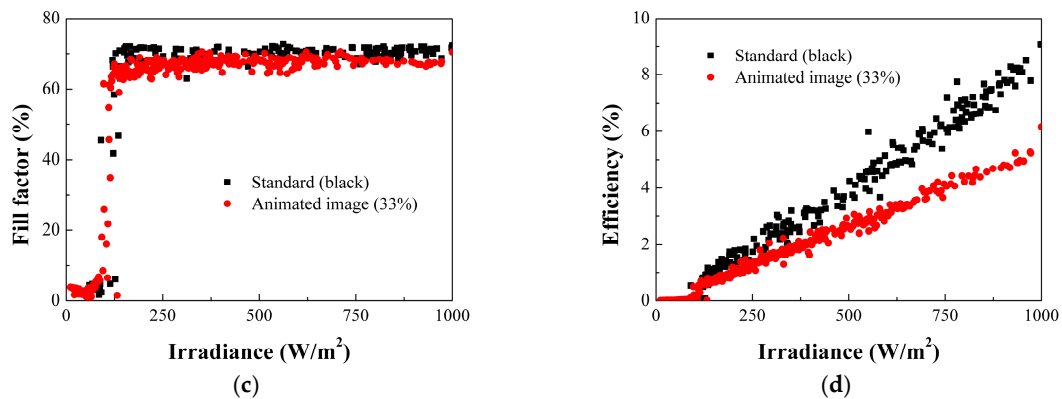


Figure 6. Cont.



**Figure 6.** Performance of the standard PV module and animated image PV module as a function of the irradiance, (a) open-circuit voltage, (b) short-circuit current, (c) fill factor, (d) conversion efficiency.

#### 4. Conclusions

Fifth-generation-sized animated image PV modules have been fabricated in this paper. A PV module with three images is demonstrated, and the images can be clearly seen from different angles. The power output of the animated image PV module is 87.6 W, which can be further improved by decreasing the see-through transmittance and increasing the number of animated images. The remarkable features of this module such as the animated image display, semitransparency, and acceptable power loss provide an option that adds a personal style and unique design to the building. This module could help improve customer acceptance and elevate the esthetic appearance of building-integrated PV modules.

**Acknowledgments:** This work is sponsored by the Ministry of Science and Technology of the Republic of China under contract Nos. 105-2632-E-212-001- and 104-2221-E-212-002-MY3.

**Author Contributions:** Yu-Chih Ou and Shui-Yang Lien designed the experiments; Yu-Chih Ou and Hsin-Yu Wu performed the experiments and measurements; Yu-Chih Ou, Hsin-Yu Wu, Chia-Hsun Hsu, Yeu-Long Jiang and Shui-Yang Lien analyzed the results; Yu-Chih Ou, Hsin-Yu Wu and Chia-Hsun Hsu wrote the paper.

**Conflicts of Interest:** The authors declare no conflict of interest.

#### References

1. Solar Power Energy. *Global Market Outlook for Solar Power 2017–2021*; Solar Power Report; SolarPower Europe: Brussels, Belgium, 2017.
2. Lee, H.M.; Yoon, J.H.; Kim, S.C.; Shin, U.C. Operational Power Performance of South-facing Vertical BIPV Window System Applied in Office Building. *Sol. Energy* **2017**, *145*, 66–77. [[CrossRef](#)]
3. Lim, J.W.; Kim, G.; Shin, M.; Yun, S.J. Colored a-Si:H Transparent Solar Cells Employing Ultrathin Transparent Multi-layered Electrodes. *Sol. Energy Mater. Sol. Cells* **2017**, *163*, 164–169. [[CrossRef](#)]
4. Myong, S.Y.; Jeon, S.W. Design of Esthetic Color for Thin-film Silicon Semi-transparent Photovoltaic Modules. *Sol. Energy Mater. Sol. Cells* **2015**, *143*, 442–449. [[CrossRef](#)]
5. Wade, N. *Art and Illusionists*, 1st ed.; Springer: Berlin/Heidelberg, Germany, 2016; ISBN 978-3-319-25229-2.
6. Je, U.; Kim, J.; Cho, H.; Lim, H.; Park, C.; Kim, G.; Park, S.; Park, Y.; Kim, K.; Woo, T.; et al. Indirect Measurement of High Grid Strip Densities over Nyquist Sampling Rate Based on the Moiré Pattern Analysis for Quality Assurance in Grid Manufacturing. *Measurement* **2016**, *91*, 634–640. [[CrossRef](#)]
7. Gauntt, D.M.; Barnes, G.T. Grid Line Artifact Formation: A Comprehensive Theory. *Med. Phys.* **2006**, *33*, 1668–1677. [[CrossRef](#)] [[PubMed](#)]
8. Vasarely, V. *Vasarely: Plastic Arts of the 20th Century*, 1st ed.; Editions Du Griffon: Neuchatel, Switzerland, 1965; ISBN 9780302002568.
9. Seder, R.B. Moveable Animated Display Device. U.S. Patent US 7151541 B2, 19 December 2006.

10. Avagliano, S.; Bianco, N.; Manca, O.; Naso, V. Combined Thermal and Optical Analysis of Laser Back-scribing for Amorphous-silicon Photovoltaic Cells Processing. *Int. J. Heat Mass Transf.* **1999**, *42*, 645–656. [[CrossRef](#)]
11. Ichikawa, Y. Fabrication Technology for Large-area a-Si Solar Cells. *Sol. Energy Mater. Sol. Cells* **1994**, *34*, 321–328. [[CrossRef](#)]
12. Berg, R.B.; Calwer, H.; Marklstorfer, P.; Meckes, R.; Schulze, F.W.; Ufert, K.D.; Vogt, H. 7% Stable Efficiency Large Area a-Si: H Solar Modules by Module Design Improvement. *Sol. Energy Mater. Sol. Cells* **1993**, *31*, 253–261.
13. Wang, J.; Wang, H.; Du, J.; Sun, R.; Xu, C.; Zhang, Y.; Wang, D.; Liu, T.; Huang, Y.; Jia, H.; et al. Performance Improvement of Amorphous Silicon See-through Solar Modules with High Transparency by the Multi-line ns-laser Scribing Technique. *Opt. Lasers Eng.* **2013**, *51*, 1206–1212. [[CrossRef](#)]
14. Bovatsek, J.; Tamhankar, A.; Patel, R.S.; Bulgakova, N.M.; Bonse, J. Thin Film Removal Mechanisms in ns-laser Processing of Photovoltaic Materials. *Thin Solid Films* **2010**, *518*, 2897–2904. [[CrossRef](#)]
15. International Electrotechnical Commission. *Thin-Film Terrestrial Photovoltaic (PV) Modules—Design Qualification and Type Approval*, 2nd ed.; International Electrotechnical Commission: Geneva, Switzerland, 2008.



© 2017 by the authors. Licensee MDPI, Basel, Switzerland. This article is an open access article distributed under the terms and conditions of the Creative Commons Attribution (CC BY) license (<http://creativecommons.org/licenses/by/4.0/>).